Optical Coherence Tomography Angiography of the Superficial Microvasculature in the Macular and Peripapillary Areas in Glaucomatous and Healthy Eyes

Henry Shen-Lih Chen,[1,2] Chun-Hsiu Liu,[1] Wei-Chi Wu,[1,2] Hsiao-Jung Tseng,[3] and Yung-Sung Lee[1]

[1]Department of Ophthalmology, Chang Gung Memorial Hospital, Linkou, Taiwan
[2]College of Medicine, Chang Gung University, Taoyuan, Taiwan
[3]Center for Big Data Analytics and Statistics, Chang Gung Memorial Hospital, Linkou, Taiwan

Correspondence: Yung-Sung Lee, Department of Ophthalmology, Chang Gung Memorial Hospital, Linkou, No. 5, Fuxing Street, Guishan District, Taoyuan City 333, Taiwan, Republic of China; nolosolee@gmail.com.

Submitted: March 12, 2017
Accepted: June 23, 2017

Citation: Chen HS-L, Liu C-H, Wu W-C, Tseng H-J, Lee Y-S. Optical coherence tomography angiography of the superficial microvasculature in the macular and peripapillary areas in glaucomatous and healthy eyes. *Invest Ophthalmol Vis Sci*. 2017;58:3637–3645. DOI:10.1167/iovs.17-21846

Purpose. To quantitatively evaluate the superficial microvasculature in the macular and peripapillary areas in glaucomatous and healthy eyes using optical coherence tomography angiography (OCT-A).

Methods. We enrolled 26 eyes of medically managed primary open-angle glaucoma patients and 27 eyes of healthy subjects were enrolled in this prospective study. Measurements of OCT-A vessel density were acquired both in the macular and peripapillary areas. We compared vessel density values, the circumpapillary retinal nerve fiber layer (cpRNFL), the ganglion cell complex (GCC), and standard automated perimetry (SAP) parameters across study groups. Areas under the receiver operating characteristic (AUROC) curves were used to evaluate diagnostic accuracy. Quadratic regression models were used to determine the correlations between SAP severity and outcome measures.

Results. The whole image vessel density (wiVD) in glaucomatous eyes was lower than that in healthy eyes in the macular (38.5% ± 2.2% vs. 43.2% ± 2.3%, $P < 0.001$) and peripapillary areas (43.8% ± 5.7% vs. 53.3% ± 3.0%, $P < 0.001$). The circumpapillary vessel density (cpVD) was also lower in glaucomatous eyes (53.3% ± 7.0% vs. 61.5% ± 3.2%, $P < 0.001$). We found the AUROCs for discriminating between glaucomatous and healthy eyes were highest for cpRNFL (0.95) and GCC (0.95); followed by macular wiVD (0.94); peripapillary wiVD (0.93); and cpVD (0.89). The correlations between SAP severity were strongest with peripapillary wiVD ($R^2 = 0.58$); followed by cpVD ($R^2 = 0.55$); GCC ($R^2 = 0.51$); cpRNFL ($R^2 = 0.42$); and macular wiVD ($R^2 = 0.36$).

Conclusions. Medically managed glaucomatous eyes show sparser superficial microvasculature in the macular area than do healthy eyes. The measurement of the macular superficial vessel density had similar diagnostic accuracy to peripapillary RNFL and macular GCC thickness for differentiating between glaucomatous and healthy eyes.

Keywords: optical coherence tomography, angiography, glaucoma, retinal vasculature

Glaucoma is a degenerative disease characterized by the progressive loss of retinal ganglion cells (RGCs) and their accompanying axons.[1] The core element in the diagnosis of glaucoma is the presence of characteristic visual field defects, but as many as 30% to 50% of RGCs may be lost before visual field deficits are detected clinically.[2,3] Therefore, a direct evaluation of RGC loss may aid in the early detection of glaucoma.[1] Traditionally, retinal nerve fiber layer (RNFL) thinning around the optic nerve head has been regarded as a measurement of RGC loss in glaucoma.

Advances in the segmentation algorithms of spectral-domain optical coherence tomography (SD-OCT) have enabled a better quantitative assessment of the ganglion cell complex (GCC), which includes the three innermost retinal layers: the RNFL; the ganglion cell layer (GCL); and the inner plexiform layer (IPL).[4] Since approximately one-half of all RGCs reside in the macula, analyzing the macular GCC using SD-OCT becomes an effective method to assess RGC loss clinically.[1,5] To date, several reports have found a high diagnostic accuracy of GCC for diagnosing glaucoma and have demonstrated that this accuracy is comparable to that of RNFL measurements.[4,6,7]

In addition to the degeneration of RGCs, there is increasing evidence that decreased ocular blood flow of the optic nerve may play an important role in the pathogenesis of glaucoma.[8–10] Radial peripapillary capillaries (RPCs), which compose a unique capillary plexus within the RNFL, constitute a critical blood source to satisfy the nutritional demands of RGC axons.[11] Although histologic studies have described the correlation between changes in RPC networks, Bjerrum scotoma, and glaucoma, in vivo studies have been limited by the lack of a technique to quantitatively characterize this microvasculature.[12,13] In this regard, optical coherence tomography angiography (OCT-A) offers insight into the perfusion status of the measured region and has been used to characterize the vasculature in various retinal layers.[14,15] Recently, researchers used OCT-A to quantify the density of perfused vessels in the optic nerve head and peripapillary region in glaucoma,[13,16–23]

and numerous lines of evidence have shown strong correlations between vessel density measurements and RNFL defects, visual field deficits, and the severity of glaucoma.[24–26] However, the superficial retinal microvasculature in the macular area in glaucoma remains unclear.

Given that RPCs are important for maintaining the normal function of RGC axons and a significant portion of RGCs reside in the macula, we hypothesized that the macular superficial microvasculature may play a critical role in the pathogenesis of glaucoma. A literature review revealed few studies concerning the macular microvasculature in glaucoma patients.[27] Therefore, the aim of the present investigation was to measure the superficial microvasculature in the macula by OCT-A in glaucomatous and healthy subjects and to clarify the relationship between vessel density and glaucoma. We also measured the vessel density in the peripapillary area; the circumpapillary RNFL (cpRNFL) thickness; and the GCC thickness to compare the diagnostic accuracy among these parameters. Finally, we evaluated the correlations between vessel density values, cpRNFL thickness, GCC thickness, and glaucoma severity. The results of this study may provide further information about the pathophysiology of glaucoma, and the identified parameters may be used to improve the diagnostic accuracy for glaucoma.

Methods

Study Design and Patient Recruitment

This prospective cross-sectional study was conducted at Chang Gung Memorial Hospital, Taiwan between June 2016 and November 2016. The study protocol was approved by the Institutional Review Board of Chang Gung Memorial Hospital and adhered to the tenets of the Declaration of Helsinki. Written informed consent was obtained from all study participants.

The study included primary open-angle glaucoma (POAG) and healthy patients who were aged older than 20 years and presented an open anterior chamber angle on gonioscopy, best-corrected visual acuity $\geq$20/25, and refractive errors less than 6 diopters. All patients underwent complete comprehensive ophthalmic examinations, including slit lamp biomicroscopy; gonioscopy; fundoscopy; intraocular pressure (IOP) measurement with Goldmann applanation tonometry; stereoscopic photography; ultrasound pachymetry (Aviso; Quantel Medical, Cournon d'Auvergne Cedex, France); and standard automated perimetry (SAP) (Humphrey Field Analyzer II; Carl Zeiss Meditec, Dublin, CA, USA). Systemic blood pressure was measured by sphygmomanometry in an upright sitting position after a 10-minute rest period. Participants with a history of hypertension and diabetes mellitus were included unless they were diagnosed with diabetic or hypertensive retinopathy.

The following exclusion criteria were used: (1) a history of intraocular surgery; (2) secondary causes of glaucoma, such as uveitis, trauma, or steroid use; (3) nonglaucomatous optic neuropathy; and (4) coexisting vitreoretinopathies or other ocular or systemic diseases known to impair the visual field. Patients with suspicious glaucomatous optic discs and/or ocular hypertension (IOP >21 mm Hg) but normal visual field tests were also excluded.

Healthy subjects were required to have normal-appearing optic discs, intact neuroretinal rims and RNFLs, IOP <21 mm Hg, and normal visual field test results, defined as a pattern standard deviation (PSD) within the 95% confidence limits and a glaucoma hemifield test (GHT) result within normal limits. The healthy subjects did not present with ocular disease except for refractive errors. In cases in which both eyes of a normal or glaucomatous patient met the inclusion criteria, only a single eye from each patient was selected at random and included in the study.

Standard Automated Perimetry

Visual fields were acquired using the Swedish Interactive Threshold Algorithm standard 30–2 strategies. Only reliable tests ($\leq$33% fixation losses, $\leq$10% false-positives, and $\leq$10% false-negatives); visual fields without rim and eyelid artifacts; and cases with no evidence that the abnormal results were caused by diseases other than glaucoma were included. Glaucoma was confirmed by the presence of at least two repeatable abnormal SAP results, which were defined as follows: (1) the GHT was outside the normal limits or PSD was significant at a $P < 5\%$ level and (2) the presence of a cluster of three or more adjacent points in typical glaucomatous locations did not cross the horizontal meridian, all of which were depressed on the pattern deviation plot at a $P < 5\%$ level and one of which was depressed at a $P < 1\%$ level on at least two consecutive plots. The severity of glaucoma was recorded as the MD value.

Optical Coherence Tomography Angiography

The optical coherence tomography angiography imaging system (AngioVue; Optovue, Inc., Fremont, CA, USA) uses an 840-nm superluminescent diode and has an A-scan rate of 70,000 scans per second. The split-spectrum amplitude-decorrelation angiography algorithm distinguishes the movement of the red blood cells in a flowing blood vessel to generate angiographic images of perfused vessels and optimize the image acquisition.[14]

Each patient underwent two imaging sessions consisting of both a 4.5 × 4.5-mm-diameter peripapillary scan centered on the optic disc and a 6.0 × 6.0-mm-diameter perifoveal scan centered at the fovea. Vessel density of the RPC in the peripapillary area was defined as extending from the internal limiting membrane (ILM) to the posterior boundary of the RNFL. Superficial vessel density in the macula was imaged from the ILM to the posterior boundary of the IPL. Vessel density was calculated by the percentage area occupied by flowing blood vessels in the selected region using the intrinsic imaging system software (Optovue, Inc.). For peripapillary scans, the whole enface image vessel density (wiVD) was measured in the entire 4.5 × 4.5-mm image, and the circumpapillary vessel density (cpVD) was measured in a 750-μm-wide elliptical annulus extending outward from the optic disc boundary (Fig. 1, top row, left). For macular scans, the wiVD was measured in the entire 6.0 × 6.0-mm image, and the parafoveal region was measured in an annulus with an outer diameter of 3 mm and an inner diameter of 1 mm (Fig. 1, top row, right).

Poor quality scans, defined as images with (1) a signal strength index of less than 45; (2) residual motion artifacts visible as an irregular vessel pattern or disc boundary on the en face angiogram; (3) RNFL segmentation errors; or (4) a local weak signal caused by medial opacities, were excluded.

For the measurements of GCC and cpRNFL, the built-in Avanti glaucoma module enabled assessment of the optic nerve head and cpRNFL and provided GCC scans. The thickness of cpRNFL was obtained along a 3.45-mm-diameter circle centered on the optic disc. The ganglion cell complex scan was centered 1-mm temporal to the fovea and covered a 6-mm-diameter circular area on the central macula. All participants underwent both OCT-A and SD-OCT imaging on the same day.

Investigative Ophthalmology & Visual Science

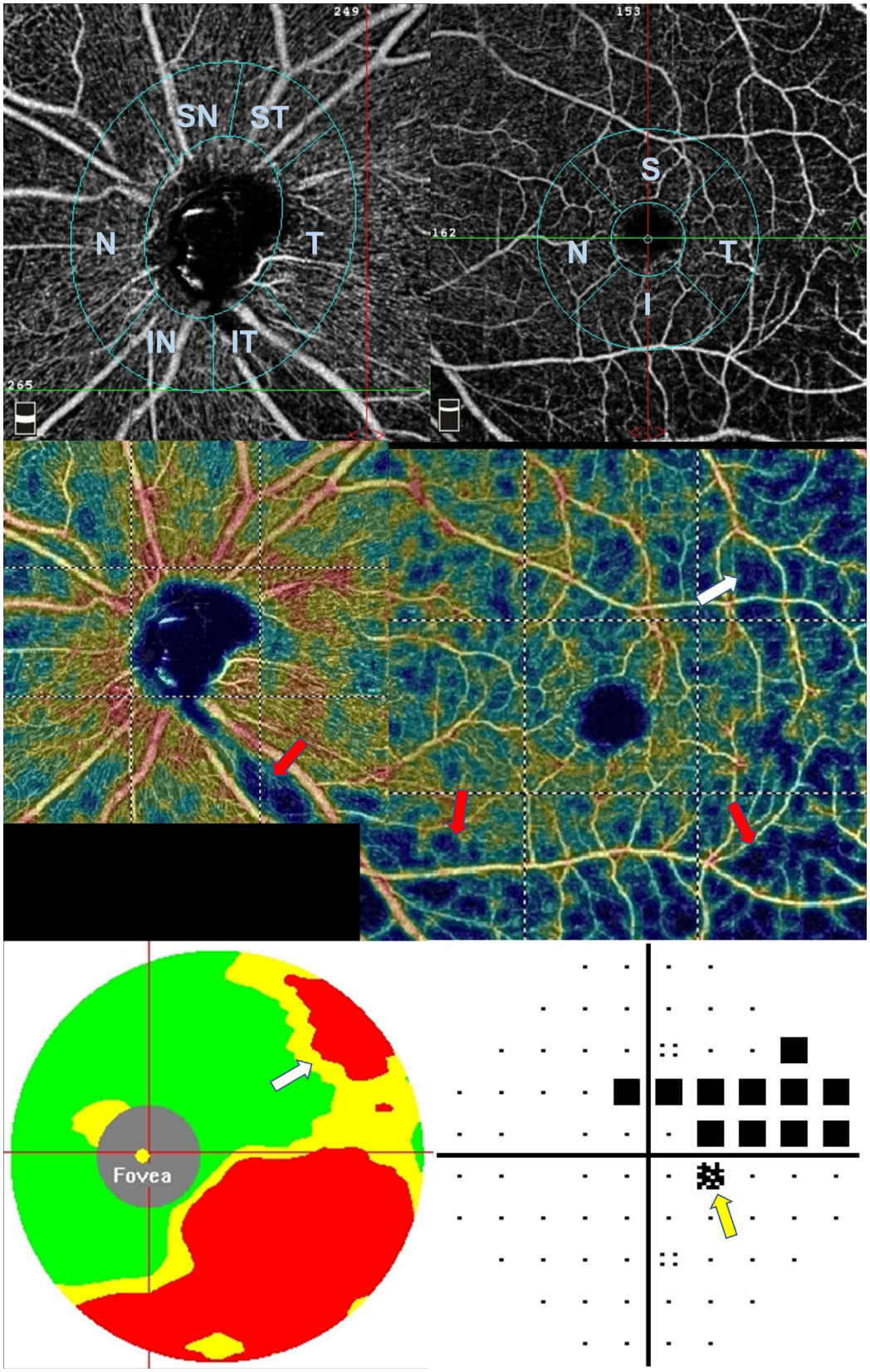

Figure 1. Left eye of a 52-year-old female with POAG. *Top row*: peripapillary and macular vessel density maps. *Second row*: montage corresponding color-coded maps. *Bottom row*: (*left*) GCC significance map; (*right*) visual field test. The superior arcuate scotoma is consistent with capillary dropout at the inferotemporal region of the peripapillary and perifoveal retina (*red arrows*). In addition, a focal capillary dropout (*white arrows*) could be seen in the superotemporal region outside the parafoveal retina. Peripapillary scanning did not detect the early changes, but the GCC map showed localized GCC thinning in the same area (*white arrows*), and the visual field results revealed early defects at the corresponding inferonasal site (*yellow arrows*). I, inferior; IN, inferonasal; IT, inferotemporal; N, nasal; S, superior; SN, superonasal; ST, superotemporal; T, temporal.

Investigative Ophthalmology & Visual Science

Table 1. Demographic and Ocular Characteristics of Healthy Subjects and Glaucoma Patients

Variable	Glaucoma Group, $n = 26$	Control Group, $n = 27$	P Value*
Demographic characteristics			
Eye: right/left, n (%)	13/13 (50.0/50.0)	15/12 (55.6/44.4)	0.69
Age, y	57 ± 13	57 ± 12	0.84
Sex, male/female, n (%)	14/12 (53.8/46.2)	15/12 (55.6/44.4)	0.90†
Clinical characteristics			
Systolic/diastolic blood pressure, mm Hg	134 ± 15/85 ± 7	121 ± 9/74 ± 9	0.001†
Diabetes mellitus, n (%)	2 (7.7)	1 (3.7)	0.61
Hypertension, n (%)	7 (26.9)	2 (7.4)	0.08
Ocular characteristics			
IOP, mm Hg	13.7 ± 2.1	13.8 ± 2.6	0.89†
CCT, μm	535 ± 29	545 ± 23	0.18†
Cup/disc area ratio	0.7 ± 0.2	0.4 ± 0.2	<0.001‡
Disc area, mm²	2.3 ± 0.4	2.3 ± 0.5	0.71‡
Rim area, mm²	0.7 ± 0.3	1.4 ± 0.4	<0.001‡
SAP MD, dB (min-max)	−8.8 ± 6.2 (−25.8 to 0.6)	0.1 ± 1.3 (−2.1 to 1.9)	<0.001‡
SAP PSD, dB (min-max)	10.4 ± 4.7 (2.3–16.9)	1.7 ± 0.1 (1.5–1.9)	<0.001‡

CCT, central corneal thickness.
* Fisher's exact test or Pearson's χ^2 test.
† Independent samples test.
‡ Mann-Whitney U test.

Statistical Analysis

Continuous variables are presented as means and standard deviations, and categorical variables are presented as frequencies and percentages. The Mann-Whitney U test and χ^2 test were used to compare the data variables between the glaucoma group and the normal control group where appropriate. Areas under the receiver operating characteristic (AUROC) curves were used to reflect the diagnostic accuracy of each parameter to differentiate between glaucomatous and healthy eyes. An AUROC of 1.0 represents perfect discrimination, whereas an AUROC of 0.5 represents chance discrimination. DeLong's test was used to test for the statistical significance of performance differences between the AUROC curves. Quadratic (curvilinear) regression models were used to evaluate the relationship between visual field severity and other variables, including macular vessel density, peripapillary vessel density, cpRNFL thickness, and GCC thickness. The results are reported as R^2 values (coefficient of determination), indicating the proportion of the variance in the dependent variable that was predictable from the independent variable. Pearson's correlation coefficient was also used to measure the strength of the relationship between paired data. The coefficient value (γ) represented weak (0.20–0.39); moderate (0.40–0.59); or strong (0.60–0.79) correlation. A value off $P < 0.05$ was considered statistically significant. All statistical analyses were performed using commercial software (Stata, version 14; StataCorp, College Station, TX, USA; and SPSS version 20.0; SPSS, Inc., Chicago, IL, USA).

Results

A total of 26 eyes of 26 POAG patients and 27 eyes of 27 healthy subjects met the criteria and were included in the analyses. There were no significant differences in eye laterality and patient sex between the two groups ($P = 0.69$ and 0.90, respectively; Table 1). The mean age at examination in the glaucoma patients and healthy subjects was 57 ± 13 years (range, 30–73) and 57 ± 12 years (range, 30–72; $P = 0.84$), respectively. Both the systolic and diastolic blood pressure values in the POAG patients were higher than those in healthy subjects ($P < 0.001$ for both). Several systemic conditions and diseases were analyzed, including heart rate, diabetes mellitus, hypertension, cardiovascular disease, and the use of systemic medications. None of these values significantly differed between the glaucoma and control groups ($P > 0.05$ for all). Regarding ocular characteristics, neither baseline IOP (13.7 ± 2.1 [range, 7–17] mm Hg versus 13.8 ± 2.6 [range, 9–18] mm Hg) nor central corneal thickness (535 ± 29 [range, 480–582] μm versus 545 ± 23 [range, 509–595] μm) differed between the glaucoma and control groups ($P = 0.89$ and 0.18, respectively). All participants (100%) in the glaucoma group were treated using at least one type of ocular antihypertensive medication at the time of OCT-A imaging, including 18 patients (69.2%) treated with prostaglandin analogues; 6 patients (23.1%) with β-adrenergic antagonists; 1 patient (3.8%) with adrenergic agonists; 1 patient (3.8%) with carbonic anhydrase inhibitors; and 8 patients (30.8%) with fixed combinations.

Peripapillary and Macular Vessel Density, cpRNFL and GCC Thickness

For vessel density in the peripapillary area, the wiVD values in glaucomatous eyes were significantly lower than those in healthy eyes (43.8% ± 5.7% vs. 53.3% ± 3.0%, $P < 0.001$). The average cpVD values in glaucomatous eyes were also lower than those in healthy eyes (53.3% ± 7.0% vs. 61.5% ± 3.2%, $P < 0.001$), especially in the inferotemporal (46.2% ± 10.9% vs. 66.4% ± 5.0%) and superotemporal quadrants (55.9% ± 10.2% vs. 66.0% ± 0.3%; $P < 0.001$ for both). Regarding vessel density in the macular area, the wiVD values in glaucomatous eyes were also lower than those in healthy eyes (38.5% ± 2.2% vs. 43.2% ± 2.3%, $P < 0.001$), but there were no significant differences in the foveal or the parafoveal area vessel density, including the average values, superior and inferior hemifield values, and any of the four quadrants ($P > 0.05$ for all). The absolute values of the differences between superior-hemi and inferior-hemi parafoveal vessel density were relatively greater in glaucomatous eyes than in healthy eyes (2.7% ± 2.1% vs. 2.2% ± 2.1%), but this difference did not reach statistical significance ($P = 0.21$; Table 2).

Table 2. Vessel Density, cpRNFL and GCC Thickness Measurements in Glaucoma and Healthy Patients

Variable	Glaucoma Group, $n = 26$	Control Group, $n = 27$	P Value*
Peripapillary vessel density, %			
Whole image	43.8 ± 5.7	53.3 ± 3.0	<0.001
Circumpapillary, average	53.3 ± 7.0	61.5 ± 3.2	<0.001
Nasal	53.2 ± 8.3	57.5 ± 5.4	0.07
Inferior nasal	51.8 ± 10.6	63.6 ± 5.3	<0.001
Inferior temporal	46.2 ± 10.9	66.4 ± 5.0	<0.001
Superior temporal	55.9 ± 10.2	66.0 ± 4.3	<0.001
Superior nasal	54.7 ± 9.5	59.2 ± 5.4	0.08
Temporal	55.3 ± 11.6	62.1 ± 4.2	0.04
Macular vessel density, %			
Whole image	38.5 ± 2.2	43.2 ± 2.3	<0.001
Fovea	19.3 ± 7.3	18.0 ± 7.9	0.64
Parafovea, average	41.9 ± 2.8	43.4 ± 3.5	0.17
Superior-hemi	42.0 ± 3.4	43.4 ± 4.1	0.24
Inferior-hemi	41.8 ± 3.3	43.3 ± 3.5	0.12
Superior-inferior difference†	2.7 ± 2.1	2.2 ± 2.1	0.21
Temporal	41.9 ± 2.9	43.4 ± 4.9	0.27
Superior	42.1 ± 4.5	44.1 ± 5.0	0.15
Nasal	41.7 ± 4.0	42.5 ± 4.4	0.63
Inferior	42.0 ± 3.5	43.5 ± 4.3	0.08
cpRNFL thickness, μm			
Average	75.8 ± 12.6	100.3 ± 7.7	<0.001
Superior	79.8 ± 16.5	101.6 ± 7.6	<0.001
Inferior	71.1 ± 12.8	98.8 ± 8.8	<0.001
GCC thickness, μm			
Average	75.7 ± 10.8	95.5 ± 7.5	<0.001
Superior	79.4 ± 15.6	96.2 ± 9.5	<0.001
Inferior	72.0 ± 11.0	94.7 ± 6.3	<0.001

* Mann-Whitney U test.
† Absolute values.

As expected, both cpRNFL thickness and GCC thickness were significantly thinner in the glaucomatous eyes than in the healthy eyes ($P < 0.001$ for all), including the average values, and the superior and inferior hemifield values (Table 2).

Diagnostic Abilities of Vessel Density, cpRNFL and GCC Thickness

Overall, the AUROC for discriminating between glaucomatous and healthy eyes was highest for cpRNFL thickness (0.95) and GCC thickness (0.95), followed by macular wiVD (0.94); peripapillary wiVD (0.93); and cpVD (0.89; Table 3; Fig. 2). The macular wiVD, peripapillary wiVD, and cpRNFL thickness showed the greatest sensitivity at 80% specificity (sensitivity: 0.92), and the GCC thickness showed the greatest sensitivity at 90% specificity (sensitivity: 0.89). Pairwise comparisons showed that the diagnostic accuracies among macular wiVD, peripapillary wiVD, cpVD, and cpRNFL and GCC thickness were similar ($P > 0.05$ for all) for differentiating between glaucomatous and healthy eyes, except for the comparison between peripapillary wiVD and cpVD. The AUROC of peripapillary wiVD (0.93) was somewhat higher than that of cpVD (0.89) and reached borderline statistical significance ($P = 0.05$).

Correlation Between Vessel Density, cpRNFL and GCC Thickness, and Visual Field Severity

The vascular-functional and structural-functional relationships between SAP-MD were strongest with peripapillary wiVD ($R^2 = 0.58$), followed by cpVD ($R^2 = 0.55$); GCC thickness ($R^2 = 0.51$); cpRNFL thickness ($R^2 = 0.42$); and macular wiVD ($R^2 = 0.36$; Fig. 3). Pearson's correlation tests showed that the peripapillary wiVD ($\gamma = 0.74$); cpVD ($\gamma = 0.73$); cpRNFL thickness ($\gamma = 0.65$); and GCC thickness ($\gamma = 0.69$) had strong positive correlations with SAP-MD ($P < 0.001$ for all) and that the macular wiVD had a moderate positive correlation with SAP-MD ($\gamma = 0.59$; $P < 0.001$). In addition, we did not find significant correlations between macular vessel density and disc area ($P = 0.10$) in this study.

Discussion

In the present investigation, we demonstrated that OCT-A vessel density, measured in the superficial layer of the retina in the macular area, distinguishes between groups of glaucomatous and healthy subjects. The macular wiVD showed a diagnostic accuracy comparable to that of other known metrics such as cpRNFL and GCC thickness for differentiating between glaucomatous and healthy eyes. We also observed a significant relationship between the superficial retinal microvasculature in the macular area and the severity of visual field damage, suggesting that a more prominently reduced OCT-A macular superficial vessel density is associated with more severe glaucoma.

Optical coherence tomography angiography has demonstrated its importance with respect to diagnosing glaucoma and understanding the pathophysiology of this disease. An attenuated microvascular network of the optic disc perfusion has been observed in subjects with glaucoma,[15,24] and Liu and colleagues[25] found reduced peripapillary retinal perfusion in

Table 3. Area Under the Receiver Operating Characteristic Curve and Diagnostic Sensitivity of Vessel Density, cpRNFL and GCC Thickness Measurements

Variable	AUROC (95% CI)	Sensitivity		P Value for Pairwise AUROC Comparison*			
		At 80% Specificity	At 90% Specificity	Peripapillary wiVD	cpVD	cpRNFL Thickness	GCC Thickness
Macular wiVD	0.94 (0.87–1.00)	0.92	0.85	0.88	0.37	0.70	0.55
Peripapillary wiVD	0.93 (0.85–1.00)	0.92	0.85		0.05	0.57	0.56
cpVD	0.89 (0.79–0.98)	0.89	0.73			0.16	0.20
cpRNFL thickness	0.95 (0.90–1.00)	0.92	0.85				0.93
GCC thickness	0.95 (0.88–1.00)	0.89	0.89				

CI, confidence interval.
* DeLong's test.

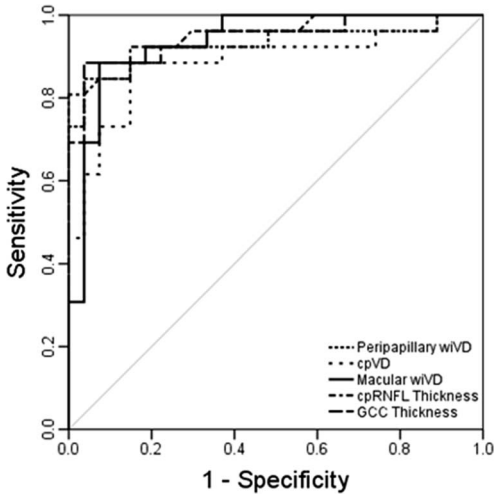

FIGURE 2. Area under the receiver operator characteristic curves of the peripapillary wiVD (0.93); cpVD (0.89); macular wiVD (0.94); cpRNFL thickness (0.95); and GCC thickness (0.95) for discriminating glaucomatous from healthy eyes.

glaucomatous eyes. These reports assessed both the superficial and deep capillary circulation and calculated blood flows in a thick retinal slab from the ILM to the retinal pigment epithelium.[15,24,25] With the advance of software in addressing image segmentation and quantification, more studies have evaluated the microvasculature in the RNFL layer, which reflects the RPCs, and reported a decreased cpVD in glaucoma patients.[17,21,22] Using OCT-A, researchers also found a lower cpVD in patients with lamina cribrosa defects and the presence of parapapillary deep-layer microvasculature dropout at the location of β-zone parapapillary atrophy.[20,23] Our current study went further and measured the superficial vessel density in the macular area to demonstrate a significant difference between glaucomatous eyes and healthy eyes. In particular, the macular superficial vessel density in glaucomatous eyes was lower than that in healthy eyes.

Measuring the macular vessel density in the diagnosis or evaluation of glaucoma has several advantages different from measuring the peripapillary vessel density. First, focal RNFL damage in early glaucoma may be more apparent in the retina farther from the peripapillary region,[28] and therefore, the peripapillary vessel density or the cpRNFL may not detect early changes, as shown in Figure 1. In addition, the myopic disc, especially in high myopia, is usually characterized by a tilted appearance and large peripapillary atrophy. The changes in the peripapillary structures may impede the discrimination between glaucomatous and normal myopic eyes. Moreover, myopic eyes have less peripapillary retinal perfusion than emmetropic eyes.[29] Wang and associates[30] reported that eyes with a tessellated fundus showed lower peripapillary retinal perfusion than eyes without a tessellated fundus, even after adjustments for sex and cpRNFL thickness, but no difference in retinal perfusion was found in the perifoveal area. Finally, the peripapillary vessel density and structural measurements, such as RNFL and optic nerve head parameters (rim, cup, etc.), have been shown to be associated with disc size.[22,31] Our study did not find a significant correlation between macular vessel density and disc size in glaucomatous eyes or healthy eyes.

In the present study, reduced macular wiVD was observed in glaucomatous eyes, but we did not find significant differences in the vessel density of the parafoveal area or the superior and inferior hemifield, and absolute values of superior-inferior differences between glaucomatous and healthy eyes. There are several possible explanations for this result. First, the larger measurement area of macular wiVD has the advantage of detecting more peripheral changes. As shown in Figure 1, vessel dropout is visible qualitatively in

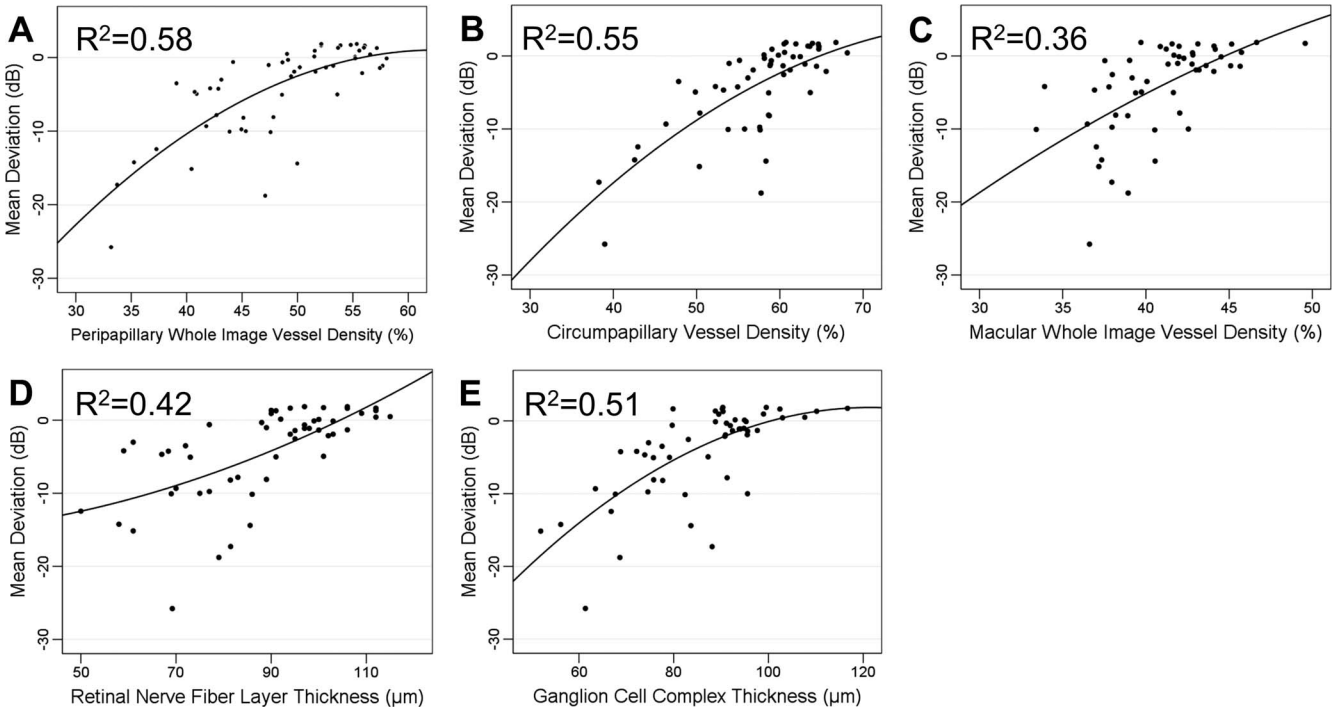

FIGURE 3. *Scatter plots* illustrating the correlation (*black curvilinear line*) (**A**) between SAP-MD and peripapillary wiVD, (**B**) SAP-MD and cpVD, (**C**) SAP-MD and macular wiVD, (**D**) SAP-MD and cpRNFL thickness, and (**E**) between SAP-MD and GCC thickness. dB, decibels; R^2, adjusted R^2 from the quadratic regression model.

the periphery outside the measurement area of the parafoveal region. It was reported that a larger measurement area of the peripapillary wiVD provides better diagnostic performance than cpVD with respect to the ability to differentiate between glaucomatous and healthy eyes.[17] In our study, the diagnostic ability of peripapillary wiVD (0.93) was also higher than that of cpVD (0.89) and reached borderline statistical significance ($P = 0.05$). Second, we enrolled glaucoma patients with visual field defects at the superior hemifield only, the inferior hemifield only, or with both superior and inferior defects into the analysis to better reflect the general population, and this heterogeneity may have offset the differences in vessel density between superior and inferior hemifields. Moreover, in eyes with visual field damage confined to a single hemifield, the vessel density in the intact hemiretinae of glaucomatous eyes was still lower than that in healthy eyes in both peripapillary and macular regions,[27] which may partially explain why the absolute values of the differences in vessel density between superior and inferior hemifields in the present study were relatively greater in glaucomatous eyes than in healthy eyes but did not reach statistical significance.

Regarding the diagnostic abilities for differentiating glaucomatous eyes from healthy eyes, our results are consistent with the findings of recent studies that have shown comparable diagnostic accuracies among vessel density, cpRNFL thickness, and GCC thickness.[17,21,25] Research has also shown that a reduction in vessel density was significantly correlated with reduced cpRNFL and GCC thickness in eyes with open-angle glaucoma.[24] However, these reports assessed the vascular parameters in the peripapillary region.[17,21,25] Our results showed that changes in macular superficial vessel density may also be a reliable diagnostic parameter for detecting glaucoma with similar sensitivities. Pairwise comparison revealed that macular wiVD had the same diagnostic power performance as other metrics.

Many studies have revealed that the vessel density measurements in the peripapillary retina are significantly correlated with cpRNFL thickness and visual field loss (either MD, PSD, or visual field index values).[19,21,22,24,25] Yarmohammadi and associates[8] also reported that decreased vessel density was significantly associated with the severity of visual field damage independent of structural loss, and the vascular-functional correlations were stronger than the standard structural (cpRNFL and rim area)-functional relationships. Furthermore, the decreased vessel density was correlated at the corresponding side of the visual field defect.[22] By using curvilinear regression analysis, our study showed not only a strong correlation between visual field severity with measurements of vessel density around the peripapillary area but also a moderate correlation with measurements of vessel density around the macular area. The reason why macular vessel density showed a relatively lower correlation with visual field severity than with peripapillary vessel density is unclear, although one possible explanation is that superficial retinal vessels in the parafoveal area are the terminal branches of retinal vessels. The vessel dropout may exhibit a stepwise decrease during the early stage of glaucoma but reach a floor during the late stage of glaucoma. Another possible reason is that the current OCT-A instrument identifies vessels on the basis of the amplitude decorrelation of blood flow, and this technique is related to blood flow over only a limited range above a certain threshold of motion. In other words, vessels with a flow below the threshold of the device are not visualized.[32] Thus, the correlated powers of the microvasculature may be limited in advanced glaucoma with extensive vessel dropout.

The strength of this study is that we measured the OCT-A vessel density in both the peripapillary area and macular area at the same time, and we also compared the diagnostic accuracy of vessel density with structural cpRNFL or GCC thickness for discriminating between healthy and glaucomatous patients. Collectively, the results of our study suggest that measures of macular vessel density may be useful for diagnosing glaucoma and evaluating disease severity. Quantifying macular superficial vessel density may be particularly useful for assessing patients with myopic optic discs, where the measures of cpRNFL are commonly influenced by disc tilting and peripapillary atrophy.

Our study also presents certain limitations. First, there is a potential confounding effect of ocular hypotensive eye drops on the hemodynamics of ocular blood flow and retinal vascular autoregulation.[33–35] Currently, five main classes of topical drugs are available in the market: beta blockers and carbonic anhydrase inhibitors decrease aqueous humor production and may be considered as "inflow" drugs; prostaglandin analogues, sympathomimetics, and miotics stimulate aqueous humor drainage and may be considered as "outflow" drugs.[36] Brimonidine is an alpha2-adrenergic receptor agonist that modulates the vasomotor response of retinal arterioles by altering nitric oxide signaling.[33] Carbonic anhydrase inhibitors may increase tissue carbon dioxide concentrations, resulting in vascular dilation and increased blood flow.[34] Prostaglandin analogues improve optic nerve head blood flow probably by a direct vasodilator effect.[35] The effects of antiglaucoma eye drops require 1 to 4 weeks to wash out,[5] and because of ethical and medical concerns, the glaucomatous patients in the current study did not stop using antiglaucoma eye drops at the time of the examination. Therefore, the glaucomatous eyes in the present study should be more precisely described as medically treated glaucomatous eyes. Nevertheless, we observed that focal decreased flow correlated with areas of glaucomatous damage, and it was not reasonable to expect a focal deficit secondary to medication use. The effect of antiglaucoma eye drops on perfusion warrants further study. Second, our study population included glaucoma patients with different severities. The small sample size in this study prevented the further subgroup analysis of glaucoma patients with different disease severities. The restricted sample size may also partially explain the lack of statistically significant differences in some sector-wise measurements of macular vessel density between glaucomatous and healthy eyes. The lack of patients with preperimetric glaucoma as a comparison group also limits the powers of our findings. Further studies with more participants to evaluate whether OCT-A has a sufficient dynamic range to provide clinically relevant information across the full spectrum of glaucoma severity are warranted. Moreover, publications have shown that the mean vessel density is significantly correlated with age range and sex.[37] In healthy eyes, macular perfusion decreased with increasing age and decreased more rapidly in males than in females.[16] Since there was no significant difference in age or sex between our study groups, there was no need for further adjustment in the current study. However, future studies should consider the variation among different study populations. Finally, since this was a cross-sectional study, we could not comment on the effectiveness of vessel density measurements in assessing disease progression. Longitudinal studies will help clarify the temporal relationships between vascular changes and glaucomatous changes in healthy participants, individuals with suspected glaucoma, and individuals with glaucoma.

In summary, glaucomatous eyes have a significantly sparser superficial vessel density in the macula than do healthy eyes, and these vessel density measurements are significantly

Investigative Ophthalmology & Visual Science

associated with the severity of visual field damage. Measurements of macular superficial vessel density show comparable diagnostic powers to other vascular or structural measurements for differentiating glaucomatous and healthy eyes. These findings offer new insights into the pathophysiology of glaucoma. Further studies excluding the effects of glaucoma medications are needed to investigate the relationship between vascular changes and glaucomatous damages.

Acknowledgments

Disclosure: **H.S.-L. Chen**, None; **C.-H. Liu**, None; **W.-C. Wu**, None; **H.-J. Tseng**, None; **Y.-S. Lee**, None

References

1. Jeoung JW, Choi YJ, Park KH, Kim DM. Macular ganglion cell imaging study: glaucoma diagnostic accuracy of spectral-domain optical coherence tomography. *Invest Ophthalmol Vis Sci*. 2013;54:4422–4429.
2. Sommer A, Katz J, Quigley HA, et al. Clinically detectable nerve fiber atrophy precedes the onset of glaucomatous field loss. *Arch Ophthalmol*. 1991;109:77–83.
3. Weinreb RN, Aung T, Medeiros FA. The pathophysiology and treatment of glaucoma: a review. *JAMA*. 2014;311:1901–1911.
4. Mwanza JC, Durbin MK, Budenz DL, et al. Glaucoma diagnostic accuracy of ganglion cell-inner plexiform layer thickness: comparison with nerve fiber layer and optic nerve head. *Ophthalmology*. 2012;119:1151–1158.
5. Cantor LB, Rapuano CJ, Cioffi GA, eds. *2014–2015 Basic and Clinical Science Course (BCSC): Section 10 Glaucoma*. Washington, DC: American Academy of Ophthalmology; 2014:40.
6. Kim HJ, Lee SY, Park KH, Kim DM, Jeoung JW. Glaucoma diagnostic ability of layer-by-layer segmented ganglion cell complex by spectral-domain optical coherence tomography. *Invest Ophthalmol Vis Sci*. 2016;57:4799–4805.
7. Garas A, Vargha P, Hollo G. Diagnostic accuracy of nerve fibre layer, macular thickness and optic disc measurements made with the RTVue-100 optical coherence tomograph to detect glaucoma. *Eye*. 2011;25:57–65.
8. Yarmohammadi A, Zangwill LM, Diniz-Filho A, et al. Relationship between optical coherence tomography angiography vessel density and severity of visual field loss in glaucoma. *Ophthalmology*. 2016;123:2498–2508.
9. Tobe LA, Harris A, Hussain RM, et al. The role of retrobulbar and retinal circulation on optic nerve head and retinal nerve fibre layer structure in patients with open-angle glaucoma over an 18-month period. *Br J Ophthalmol*. 2015;99:609–612.
10. Grunwald JE, Piltz J, Hariprasad SM, DuPont J. Optic nerve and choroidal circulation in glaucoma. *Invest Ophthalmol Vis Sci*. 1998;39:2329–2336.
11. Yu PK, Balaratnasingam C, Xu J, et al. Label-free density measurements of radial peripapillary capillaries in the human retina. *PLoS One*. 2015;10:e0135151.
12. Yu PK, Cringle SJ, Yu DY. Correlation between the radial peripapillary capillaries and the retinal nerve fibre layer in the normal human retina. *Exp Eye Res*. 2014;129:83–92.
13. Mansoori T, Sivaswamy J, Gamalapati JS, Agraharam SG, Balakrishna N. Measurement of radial peripapillary capillary density in the normal human retina using optical coherence tomography angiography. *J Glaucoma*. 2017;26:241–246.
14. Jia Y, Tan O, Tokayer J, et al. Split-spectrum amplitude-decorrelation angiography with optical coherence tomography. *Opt Express*. 2012;20:4710–4725.
15. Jia Y, Wei E, Wang X, et al. Optical coherence tomography angiography of optic disc perfusion in glaucoma. *Ophthalmology*. 2014;121:1322–1332.
16. Yu J, Jiang C, Wang X, et al. Macular perfusion in healthy Chinese: an optical coherence tomography angiogram study. *Invest Ophthalmol Vis Sci*. 2015;56:3212–3217.
17. Yarmohammadi A, Zangwill LM, Diniz-Filho A, et al. Optical coherence tomography angiography vessel density in healthy, glaucoma suspect, and glaucoma eyes. *Invest Ophthalmol Vis Sci*. 2016;57:OCT451–OCT459.
18. Leveque PM, Zeboulon P, Brasnu E, Baudouin C, Labbe A. Optic disc vascularization in glaucoma: value of spectral-domain optical coherence tomography angiography. *J Ophthalmol*. 2016;2016:6956717.
19. Mammo Z, Heisler M, Balaratnasingam C, et al. Quantitative optical coherence tomography angiography of radial peripapillary capillaries in glaucoma, glaucoma suspect, and normal eyes. *Am J Ophthalmol*. 2016;170:41–49.
20. Suh MH, Zangwill LM, Manalastas PI, et al. Optical coherence tomography angiography vessel density in glaucomatous eyes with focal lamina cribrosa defects. *Ophthalmology*. 2016;123:2309–2317.
21. Scripsema NK, Garcia PM, Bavier RD, et al. Optical coherence tomography angiography analysis of perfused peripapillary capillaries in primary open-angle glaucoma and normal-tension glaucoma. *Invest Ophthalmol Vis Sci*. 2016;57:OCT611–OCT620.
22. Akagi T, Iida Y, Nakanishi H, et al. Microvascular density in glaucomatous eyes with hemifield visual field defects: an optical coherence tomography angiography study. *Am J Ophthalmol*. 2016;168:237–249.
23. Suh MH, Zangwill LM, Manalastas PI, et al. Deep retinal layer microvasculature dropout detected by the optical coherence tomography angiography in glaucoma. *Ophthalmology*. 2016;123:2509–2518.
24. Wang X, Jiang C, Ko T, et al. Correlation between optic disc perfusion and glaucomatous severity in patients with open-angle glaucoma: an optical coherence tomography angiography study. *Graefes Arch Clin Exp Ophthalmol*. 2015;253:1557–1564.
25. Liu L, Jia Y, Takusagawa HL, et al. Optical coherence tomography angiography of the peripapillary retina in glaucoma. *JAMA Ophthalmol*. 2015;133:1045–1052.
26. Lee EJ, Lee KM, Lee SH, Kim TW. OCT angiography of the peripapillary retina in primary open-angle glaucoma. *Invest Ophthalmol Vis Sci*. 2016;57:6265–6270.
27. Yarmohammadi A, Zangwill LM, Diniz-Filho A, et al. Peripapillary and macular vessel density in patients with glaucoma and single-hemifield visual field defect. *Ophthalmology*. 2017;124:709–719.
28. Leung CK, Lam S, Weinreb RN, et al. Retinal nerve fiber layer imaging with spectral-domain optical coherence tomography: analysis of the retinal nerve fiber layer map for glaucoma detection. *Ophthalmology*. 2010;117:1684–1691.
29. Wang X, Kong X, Jiang C, Li M, Yu J, Sun X. Is the peripapillary retinal perfusion related to myopia in healthy eyes? A prospective comparative study. *BMJ Open*. 2016;6:e010791.
30. Wang X, Zheng Y, Kong X, Zhu L, Sun X. The characteristics of peripapillary retinal perfusion by optical coherence tomography angiography in tessellated fundus eyes. *PLoS One*. 2016;11:e0159911.
31. Budenz DL, Anderson DR, Varma R, et al. Determinants of normal retinal nerve fiber layer thickness measured by Stratus OCT. *Ophthalmology*. 2007;114:1046–1052.
32. Tokayer J, Jia Y, Dhalla AH, Huang D. Blood flow velocity quantification using split-spectrum amplitude-decorrelation angiography with optical coherence tomography. *Biomed Opt Express*. 2013;4:1909–1924.
33. Feke GT, Bex PJ, Taylor CP, et al. Effect of brimonidine on retinal vascular autoregulation and short-term visual function

Investigative Ophthalmology & Visual Science

in normal tension glaucoma. *Am J Ophthalmol*. 2014;158:105–112.e1.

34. Siesky B, Harris A, Brizendine E, et al. Literature review and meta-analysis of topical carbonic anhydrase inhibitors and ocular blood flow. *Surv Ophthalmol*. 2009;54:33–46.
35. Tsuda S, Yokoyama Y, Chiba N, et al. Effect of topical tafluprost on optic nerve head blood flow in patients with myopic disc type. *J Glaucoma*. 2013;22:398–403.
36. Bucolo C, Platania CB, Reibaldi M, et al. Controversies in glaucoma: current medical treatment and drug development. *Curr Pharm Des*. 2015;21:4673–4681.
37. Coscas F, Sellam A, Glacet-Bernard A, et al. Normative data for vascular density in superficial and deep capillary plexuses of healthy adults assessed by optical coherence tomography angiography. *Invest Ophthalmol Vis Sci*. 2016;57:OCT211–OCT223.

Investigative Ophthalmology & Visual Science